

The absolute sensitivity of digital colour cameras

Fred Sigernes^{1,*}, Margit Dyrland¹, Nial Peters¹, Dag Arne Lorentzen¹, Trond Svenøe²,
Karsten Heia³, Sergey Chernouss⁴, Charles Sterling Deehr⁵ and Mike Kosch⁶

¹ The University Centre in Svalbard (UNIS), N-9171 Longyearbyen, Norway

² Energy Campus Nord, Hammerfest, Norway

³ The Norwegian Institute of Food, Fisheries and Aquaculture Research, Tromsø, Norway

⁴ Polar Geophysical Institute, Murmansk Region, Apatity, Russia

⁵ Geophysical Institute, University of Alaska, Fairbanks, USA

⁶ Communication Systems, Lancaster University, Lancaster LA1 4WA, UK

*fred@unis.no

Abstract: A new and improved method to obtain the average spectral pixel responsivity and the quantum efficiency of Digital Single Lens Reflex (DSLR) cameras is outlined. Two semi-professional cameras, the Nikon D300 and the Canon 40D, are evaluated. The cameras red, green and blue pixel responsivities and quantum efficiency are retrieved by illuminating an integrating sphere with a wavelength tunable monochromator. 31 intensity calibrated monochromatic spectral lines from 4000 to 7000 Å, with a bandpass of ~12 Å, were used as a library to solve the main equations of observation for the cameras. Both cameras have peak sensitivity in the blue and minimum sensitivity in the red. The Canon 40D has blue and green channel sensitivity close to the Nikon D300. The Canon red channel has half the sensitivity of the Nikon camera.

©2009 Optical Society of America

OCIS codes: (120.4800) Optical Standards and testing; (300.6550) Spectroscopy, visible; (150.1488) Calibration; (350.0350); Astronomical optics; (350.6090) Space optics.

References and links

1. F. Sigernes, J. M. Holmes, M. Dyrland, D. A. Lorentzen, T. Svenøe, K. Heia, T. Aso, S. Chernouss, and C. S. Deehr, "Sensitivity calibration of digital colour cameras for auroral imaging," *Opt. Express* **16**(20), 15623–15632 (2008).
2. D. Baker, and G. Romick, "The Rayleigh: interpretation of the unit in terms of column emission rate or apparent radiance expressed in SI units," *Appl. Opt.* **15**(8), 1966–1968 (1976).
3. F. Sigernes, J. M. Holmes, M. Dyrland, D. A. Lorentzen, S. Chernouss, T. Svenøe, J. Moen, and C. S. Deehr, "Absolute calibration of optical devices with a small field of view," *J. Opt. Technol.* **74**, 669–674 (2007).
4. R. Berry, and J. Burnell, "Measuring CCD performance" in *Handbook of Astronomical Image Processing*, (Willmann-Bell, Inc., 2006), pp. 227–248.

1. Short background

The main motivation for this work is to develop a method to obtain the spectral responsivity or the quantum efficiency of each pixel in a Digital Single Lens Reflex (DSLR) camera. These cameras have become valuable tools for studies of the night sky including phenomena such as aurora and airglow. It is therefore essential to establish a method to quantify the light throughput of the cameras. Even though our focus is on the aurora, the results should be of interest to other fields of science such as astronomy, remote sensing and industrial processing as well.

The method presented here is an improvement of work already published in this journal [1], where a low intensity light source tunable in wavelength was described using a Lambertian screen as the target surface for the DSLR cameras. As promised, we have now

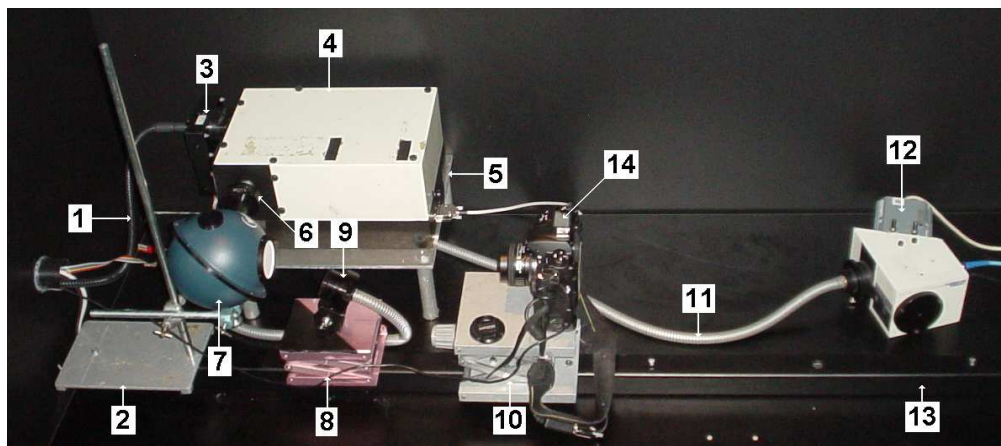


Fig. 1. Experimental setup: (1) fiber bundle from lamp located in neighboring room, (2) mount / stand for integrating sphere, (3) order sorting filter wheel in front of entrance slit, (4) Jobin Yvon HR320 monochromator, (5) table, (6) exit slit plane, (7) Edmund Scientific integrating sphere, (8) laboratory lift table, (9) fiber bundle holder, (10) camera table, (11) fiber bundle used as input to spectrograph, (12) Oriel FICS 7743 spectrograph, (13) optical mount rail, and (14) DSLR camera with normal 50 mm f/1.4 objective.

improved the experimental setup by replacing the screen with an integrating sphere to obtain a more uniform illumination source as a function of wavelength. It is now possible to calculate the average pixel sensitivity instead of the total sensitivity of the cameras.

Results from two semi-professional DSLR cameras, the Nikon D300 and the Canon 40D, are presented and evaluated. Both cameras were announced in August 2007 and cost approximately the same. Note that there is no negative or positive bias towards any manufacturer of DSLR cameras; we simply choose what is available based on price and availability.

2. The experimental setup

Figures 1 and 2 show the updated experimental setup and the optical diagram of the system, respectively. Each optical part is identical and described in detail in [1], except the integrating sphere that replaces the flat Lambertian surface. The main components are a fiber illuminator (Leica 150W) that is connected to the entrance slit of a monochromator (Jobin Yvon HR320). The diffracted light at the exit slit of the monochromator is then fed into the integrating sphere. The output of the sphere is the target for both the DSLR cameras and the intensity calibrated FICS spectrograph (Fixed Compact Spectrograph from Oriel SN 7743).

The sphere, from Edmund Optics, is designed to integrate radiant light fluxes. The sphere is 6 inches in diameter. Its interior walls are coated with Spectralon that has a diffuse reflectance factor of 0.98 throughout the visible part of the spectrum. The monochromatic light that enters the 1 inch diameter input port of the sphere is scattered multiple times before it exits the 2.5 inch diameter output port.

In addition, a transmitting diffuser is used at the output port of the integrating sphere to diffuse the light even more (see Fig. 2). The diffuser is 0.5 mm thick and made of Teflon (opal). This was found necessary due to the fact that the first region of illumination in the sphere, caused by reflected light directly from the exit slit of the monochromator, is easily seen from the output port. This illuminated region is rather large compared to the diameter of the sphere. The effect was clearly seen even at relatively small off-axis view angles to the output port.

Finally, the net result is a uniform illuminated surface that is comparable to the Lambertian surface that is used for calibrating narrow field of view instruments such as our spectrograph [3]. The field of view of the spectrograph is fully illuminated by an area that is

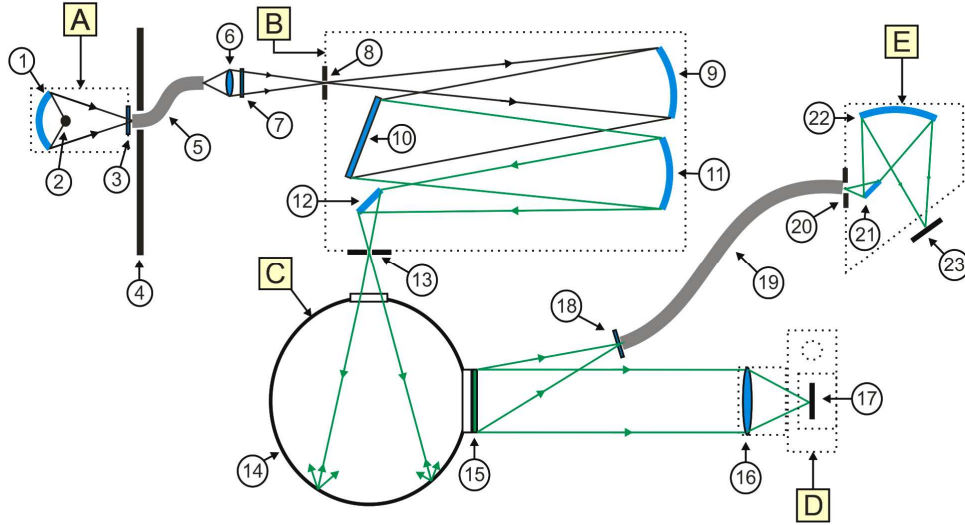


Fig. 2. Optical diagram. [A] Leica 150W fiber illuminator: (1) mirror, (2) Tungsten filament, (3) heat filter, (4) blocking wall, and (5) fiber bundle. [B] Jobin Yvon HR320 Monochromator: (6) f-matching lens, (7) order sorting filter, (8) entrance slit, (9) collimator mirror, (10) plane reflective grating, (11) focusing mirror, (12) flat surface folding mirror, and (13) exit slit. [C] Edmund Scientific General purpose 6 inch diameter integrating sphere: (14) sphere, and (15) transmitting diffuser (Teflon). [D] DSLR camera: (16) 50 mm normal f/1.4 objective, and (17) CMOS / CCD detector. [E] Oriel FICS 7743 spectrograph: (18) order sorting filter, (19) fiber bundle, (20) entrance slit, (21) folding mirror, (22) concave grating, and (23) CCD detector.

uniform in intensity, and equal to the corresponding area that fills the field of view of each selected pixel of the cameras. As long as the field of view of the pixels and the spectrograph are filled neither the look angle nor the distance to the diffuser matters. The changing sizes of the pixel fields of view at the diffuser surface compensates exactly for both the changing distances and angles.

Both the Nikon D300 and the Canon 40D cameras are operated in manual mode with sensitivity set at ISO 1600. The Nikon D300 uses a Nikon 50mm f/1.4 AF-D lens, while the Canon 40D uses the Canon EF 50mm f/1.4 USM lens. The lenses are operated at maximum aperture (f-value set to 1.4). Exposure times between 3 and 4 seconds were chosen to avoid overexposures.

3. The spectral pixel responsivity

The assembled wavelength tunable system is designed for the visible part of the spectrum (4000-7000 Å), producing monochromatic lines with a bandpass of ~12 Å. The calibrated FICS spectrograph measures the intensity of the integrating sphere output in units of R/Å [2]. The bandpass of the spectrograph is $\Delta\lambda \approx 100$ Å. As result, the spectral responsivity for each camera is calculated using all 31 spectra and images [1]. The equation of observations is

$$\hat{u}^{(k)} = C \cdot \hat{S}^{(k)} \cdot \Delta\lambda, \text{ [CTS / s]} \quad (1)$$

where the subscript $k \in [R, G, B]$ labels the Red, Green and Blue channels of the transparent Colour Filter Mosaic filter (CFM) in front of each pixel of the sensor, respectively. The vector $\hat{u}^{(k)}$ contains 31 numbers of averaged pixel raw counts per second for each colour channel, k . The matrix C is given as

$$C = [C_1 C_2 C_3 \dots C_{31}]^T \cdot [\text{R}/\text{Å}] \quad (2)$$

Each vector C_i , $i \in [1 \dots 31]$ contains the spectrum as measured by the FICS spectrograph.

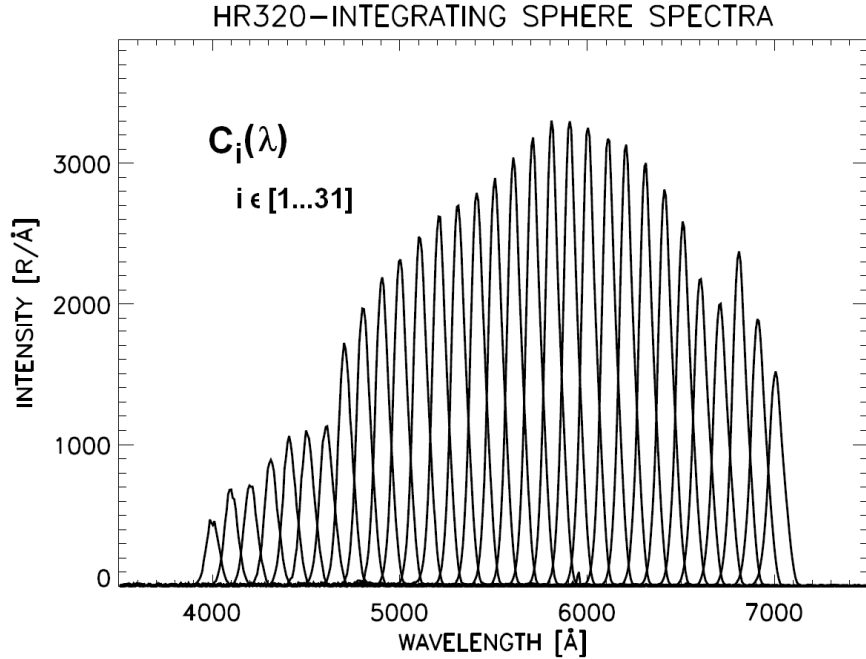


Fig. 3. Sphere source functions. $C_i(\lambda)$ is the set of observations that consists of 31 spectra from the monochromator (HR320) illuminating the 6 inch diameter integrating sphere from Edmund Optics.

The dimension of the spectra is reduced to 31 by re-sampling at each center wavelength setting of the monochromator. The spectral responsivity $\hat{S}^{(k)}$ is now found by solving Eq. (1) by Singular Value Decomposition (SVD).

4. The quantum efficiency

Another way to characterize the spectral sensitivity of a camera is to calculate the Quantum Efficiency (QE). It is defined as the fraction of photons that will generate electrons detectable by the photo-reactive sensors. In our case with monochromatic source functions in units of $R/\text{\AA}$, the QE may be expressed as

$$QE_i^{(k)} \approx \left[\frac{4\pi \cdot u_i^{(k)} \cdot \Delta t \cdot g}{10^6 C_i \cdot \Delta \lambda \cdot \Delta A} \right] \times 100, [\%] \quad (3)$$

where ΔA is the pixel area in units of cm^2 , Δt is the exposure time in seconds and g is the gain of the detector defined as the conversion factor between the number of electrons and raw counts per pixel. A simple procedure of how to measure the gain is given by [4]. At ISO 1600 the gain is 0.775 and 0.675 electrons per 12-bit data count for the 40D and the D300, respectively.

5. Calibration results

Our new library of calibrated spectra is shown in Fig. 3. The intensity of the output port of the integrating sphere rises from $\sim 500 R/\text{\AA}$ at 4000\AA to a maximum of $\sim 3300 R/\text{\AA}$ at 5800\AA , reducing to $\sim 1500 R/\text{\AA}$ at 7000\AA . The dips at 4600\AA and 6700\AA are due to drops in the grating efficiency of the monochromator. Note that the intensity is equal in shape and twice as bright as the Lambertian screen setup described in [1]. This is expected, since we apply the

same monochromator as the input source and the sphere is more effective than the screen to integrate the incoming radiation.

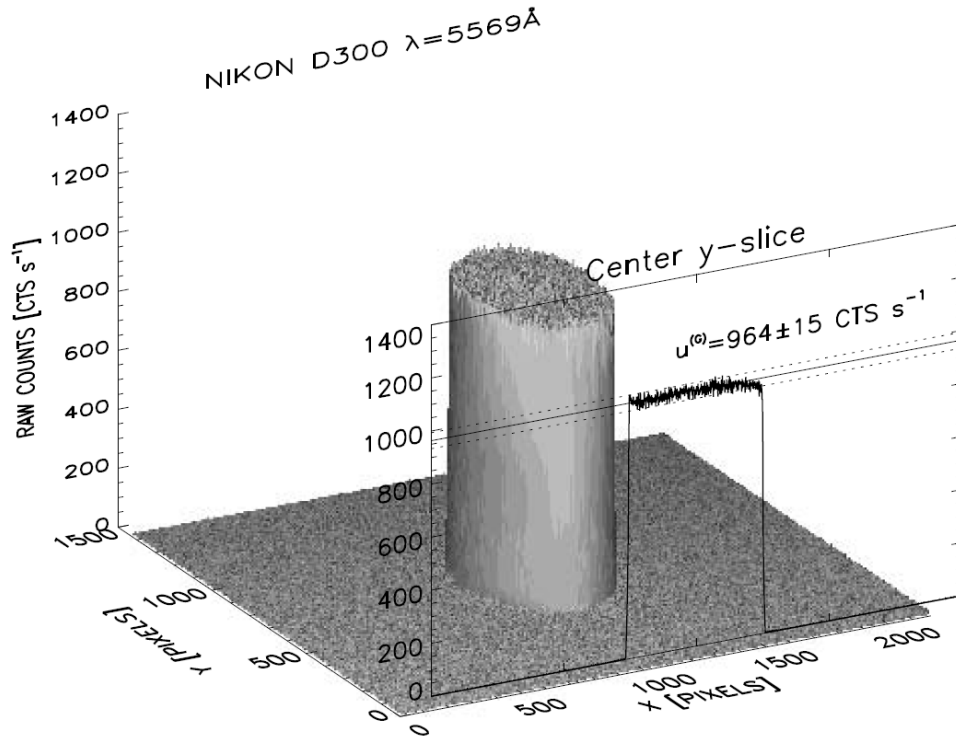


Fig. 4. Raw counts from the Nikon D300. Exposure time is 3 seconds at ISO 1600 with a 50 mm normal objective fixed at $f/1.4$. The shaded surface represents the green channel 12-bits raw counts per second. The source is a monochromatic illuminated sphere at center wavelength 5569 Å. The center y-axis slice of the surface is shown together with the calculated height of the plateau (solid horizontal line) and the 2σ standard deviation (dotted lines).

Figure 4 shows the Nikon D300 green channel raw counts per second when the sphere is illuminated with light at 5569 Å center wavelength. Note that dark frame subtraction is carried out to reduce the background level. The resulting image is shaped like a steep mountain cliff with a sharp leveled circular plateau. The height of the plateau is used as the average pixel raw count response. The plateau height is calculated by selecting raw count values within a 200x200 pixel square area in the center of the image. Using the notation in Section 3, the plateau height is $u^{(g)} = 964$ CTS/s. The corresponding standard deviation is $2\sigma = \pm 30$ CTS/s, which in percentage terms is close to 3% variation across the plateau. The 2σ deviation is compatible with Poisson statistics where noise is defined as the square root of the counts. The calculated values are visualized in Fig. 4 by plotting the center y-axis slice of the mountain cliff. The result looks like a square pulse with ripple noise on the top that is within the calculated deviation. The output of the sphere is, in other words, sufficiently uniform to assume that the above 200x200 pixel average is the same for all pixels.

The next step is to repeat the procedure to obtain the average raw counts per second as a function of wavelength for each color channel of the cameras. The first thing we noticed when handling the raw data from the Canon 40D is that the counts are fixed at 14-bits resolution. The range is, in other words, from 0 to 16383 counts. The Nikon D300 has a 12-bit range (0 – 4095 counts). As a consequence, the 40D counts are scaled down by a factor of (1/4) in order to be comparable to the D300. The D300 was first operated at 3 seconds exposures with no

overexposures occurring as we changed the wavelength of the monochromator. At 4 seconds the green channel became overexposed. On the other hand, the Canon 40D did not overexpose

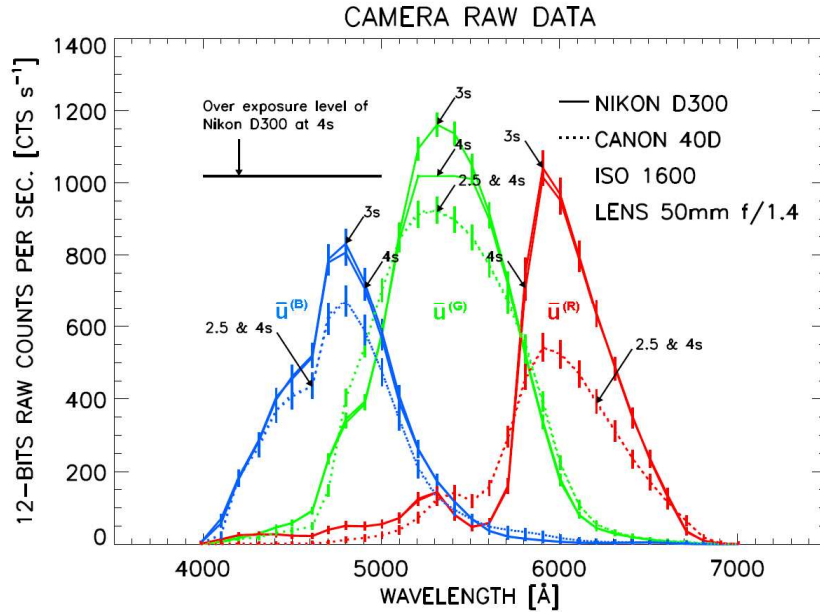


Fig. 5. Camera raw data. Solid lines are the raw counts per second from the Nikon D300 camera for each color channel (Red, Green and Blue). The dotted lines are the corresponding data from the Canon 40D camera. Each curve is labeled with exposure time settings of the cameras. Both cameras were operated with identical settings using normal objective lenses (50mm f/1.4) at ISO 1600. The error bars represent the 2σ standard deviation of the count rates.

at 4 seconds exposure time. It also turned out that we could not set the exposure time of the 40D to 3 seconds. Only 2.5, 3.2 and 4 second intervals were possible. The procedure was therefore repeated to make sure that we obtain the same counts per second for all intervals.

Figure 5 shows the resulting raw counts per second obtained with variable exposure intervals for both cameras. It is hard to see any difference between the curves as a function of exposure time for each camera alone, especially for the 40D. The only difference appears when the D300 green channel is overexposed at 4 seconds. The effect is seen comparing the 3 and 4 second exposures. The peak of the 4 second exposure looks like it has been cut off compared to the 3 second one in the 5200 to 5500 Å wavelength region. Also notice that the error bars become zero in this region. This is expected since the error bars are defined as the 2σ standard deviation of the count rates. The D300 blue and red channel count rates are almost identical, with deviations that are well within the error bars. It is therefore reasonable to assume that the raw count rates are constant as a function of exposure time in the interval $\sim(3-4)$ seconds for both cameras.

The count rate profiles of the cameras shown in Fig. 5 are quite similar in shape, especially the blue and red channels. However, the 40D green channel profile is slightly more symmetric than the corresponding D300 profile. This is due to the fact that the 40D green counts are little bit higher than the D300 green counts in the 4800 to 5100 Å wavelength region. The same is seen in the 5400 to 5800 Å wavelength region when comparing the red channels.

Both cameras have peak count rates in the green channels. However, the D40 has a higher blue than red peak count rate, while this is vice versa for the D300. What this means, in terms of difference in color balance between the cameras, depends on the spectral responsivity or

the quantum efficiency. The raw count rate profiles alone are not sufficient in order to conclude on this issue.

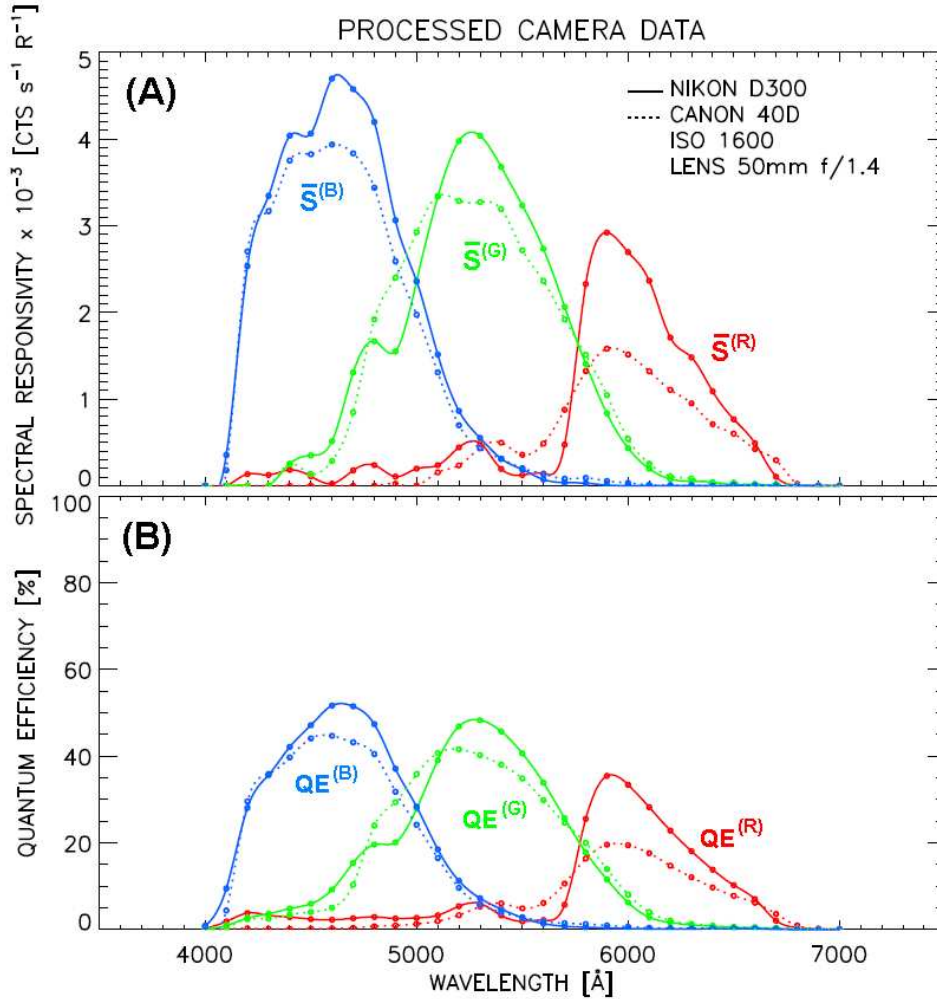


Fig. 6. Processed camera data. Panel (A): Solid lines are the spectral responsivity of the Nikon D300 camera for each color channel (Red, Green and Blue). The dotted lines are for the Canon 40D camera. Panel (B) shows the corresponding calculated quantum efficiency. Both cameras were operated with identical settings using normal objective lenses (50mm f/1.4) at ISO 1600.

If we define the width of the profile for each color channel to be the wavelength region where it has equal to, or greater than, half of its maximum count rate, then it is clear that the D40 has wider profiles than the D300 for all color channels. The D40 profile is ~ 250 Å wider than the D300 in the green channel. The corresponding blue and red differences in widths are 70 and 160 Å, respectively.

The main difference between the cameras becomes evident in the level of the count rates. The Nikon D300 count rates are generally higher when compared to the Canon 40D, except for the wavelength regions mentioned above. By integration we find that the D300's blue, green and red channels have ~ 16 , 8 and 50% higher count rates compared to the D40, respectively

The spectral responsivity and the quantum efficiency may now be solved according to Eqs. (1) and (3), respectively. Based on the above findings, the 3 second exposure by the

D300 and the 4 second exposure by the 40D camera are chosen to represent the raw count rates in the calculations. The net result is shown in Fig. 6 for both cameras.

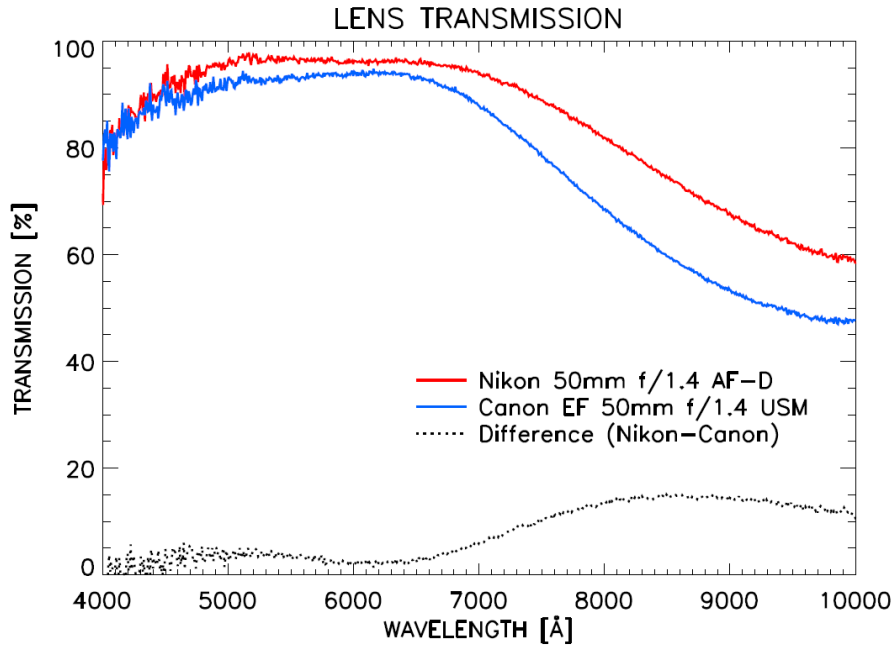


Fig. 7. Normal objective spectral lens transmissions for the Nikon 50mm f/1.4 AF-D (red solid line) and the Canon EF 50mm f/1.4 USM (blue solid line). The dotted black line is the difference in transmission between the Nikon and Canon lens, respectively.

The calculated spectral responsivities and the quantum efficiency curves are compatible in shape and amplitude. Note that the quantum efficiency calculation is a more direct and robust method since it does not depend on the Singular Value Decomposition. It is now clear that both cameras have their peak sensitivity in the blue and minima in the red channels. The color balance between the channels is, in other words, the same for both cameras. However, as expected from the level of the count rate profiles, the Nikon D300 is the most sensitive camera. The D300 has a peak quantum efficiency of 50% and spectral responsivity of $4.3 \times 10^{-3} \text{ counts s}^{-1} \text{ R}^{-1}$ in the blue channel at 4600 Å. The green channel quantum efficiency peaks at 48% with $3.9 \times 10^{-3} \text{ counts s}^{-1} \text{ R}^{-1}$ in spectral responsivity at 5300 Å, while the red channel peak is lowest at 35% and $2.8 \times 10^{-3} \text{ counts s}^{-1} \text{ R}^{-1}$ at 5900 Å. Again, by integration we find that the D300's blue, green and red channels have ~17, 9 and 54% higher spectral responsivity compared to the D40, respectively. The corresponding difference in quantum efficiency is 11, 3 and 47%.

The above is a surprising result. We double checked our experimental setup to make sure that we actually used the same settings on both cameras. Also note that, the total difference between the two sets of source functions used to obtain the spectral responsivity and quantum efficiency only varied by $\pm 17 \text{ R}/\text{Å}$. The difference is so small that it is hard to see it if we overlay the curves of the 40D source functions in Fig. 3.

One factor that could explain the discrepancy, especially in the red, could be the difference in the spectral transmission of the lenses. The Nikon 50mm f/1.4 AF-D and the Canon EF 50mm f/1.4 USM lenses are almost identical with the same number of optical elements in the lens construction. Figure 7 shows the spectral transmission profiles using the FICS spectrograph as the detector and a flat Lambertian surface as the target reference. The surface was illuminated by a Tungsten lamp. The lenses were mounted in front of the spectrograph's

entrance fiber bundle. The setup is identical to our narrow field of view intensity calibration procedure [3]. The shape of the transmission profiles is more or less equal for both lenses. There is a gradual increase from ~80% at 4000 Å up to a more stable region above ~90% from 4500 to 6500 Å. In the deep red part of the spectrum ($\lambda > 6500$ Å), the transmission factors start to decrease more rapidly to a level below ~50 to 60% at 10 000 Å. The Nikon lens is overall more effective than the Canon lens throughout the visible region (4000 – 7000 Å) and the near infra-red (7000 - 10000 Å) by a factor of ~5 and 15%, respectively.

If we take into account the transmission of the lenses, the difference between the cameras in spectral responsivity and quantum efficiency is only changed by a few percent. The D300's blue, green and red channels now have ~12, 5 and 50% higher spectral responsivity compared to the D40, respectively. The updated differences in quantum efficiency become ~7% for the blue, 0% for the green and 45% for the red channels.

The above result indicates that the main difference between these two cameras is in their detectors. Both cameras use a CMOS (Complementary Metal Oxide Semiconductor) sensor and a Color Filter Mosaic (CFM) to separate the colors. The main difference in spectral responsivity is found to be in the red channels, and could well be related to the transmission of the red elements in the CFM, the infra-red filter or in the semiconductors used. This is an interesting topic, but it is beyond the scope of this paper.

A digital camera image could contain more information than just relative scaled intensities or color coded pixel values that have little physical meaning in terms of brightness on a quantitative scale. The recent improvements in both sensitivity and dynamic range enable the DSLR camera to be used as an intensity tool as well. But the lesson learned from this exercise is that there seems to be a lack of a common standard for camera sensitivity given by the manufacturers. As shown above for Nikon and Canon, the ISO (International Organization for Standardization) values, originally defined as the speed of photographic film, may not be the optimum parameter representing the sensitivity of a digital sensor. The spectral responsivity or the quantum efficiency is the parameter that should be used in the future to characterize the sensitivity of a camera. We hope that the manufacturers can provide this information in future. It would increase the usage and potential of these fantastic devices.

6. Concluding remarks

The principal results obtained by this study can be summarized as follows.

- (1) A fiber optical lamp is connected to the input of a monochromator which is tunable in wavelength in the visible part of the electromagnetic spectrum (4000 – 7000 Å). The output of the monochromator illuminates an integrating sphere with a bandpass of ~12 Å.
- (2) The brightness of the sphere is monitored by an intensity calibrated spectrograph. A library of source functions consisting of 31 monochromatic lines is obtained in the visible part of the electromagnetic spectrum. The intensities range from ~500 to 3300 R/Å.
- (3) The intensity of the sphere is sufficiently uniform to obtain the average pixel response for each colour channel of a digital colour camera. As a result, it is possible to retrieve the spectral responsivity and the quantum efficiency of each pixel as a function of wavelength.
- (4) Two semi-professional DSLR cameras, the Nikon D300 and Canon 40D, have been calibrated. The sensitivities based on calculations of spectral responsivity and quantum efficiency, are found to be higher in the blue compared to the green and red channels. The Nikon D300 has a peak quantum efficiency of 50% at 4600 Å, 48% at 5300 Å and 35% at 5900 Å. The corresponding spectral responsivity is found to be 4.3×10^{-3} , 3.9×10^{-3} and 2.8×10^{-3} in units of counts $s^{-1} R^{-1}$. The D300 is slightly more

sensitive than the 40D in the blue and green channels. The main difference is found in the red channel. The 40D is up to 50% less red sensitive than the D300.

- (5) The ability of a DSLR camera to measure intensity of light in terms of absolute physical units opens up new possibilities. A standard measure such as the quantum efficiency or spectral responsivity could be part of a certificate provided by the manufacturer in the future.

Acknowledgement

This work was financially supported by The Research Council of Norway through the project named: Norwegian and Russian Upper Atmosphere Co-operation On Svalbard #178911/S30 (NORUSCA).